Diagrammatic approach to non-Gaussianity from inflation

Christian T. Byrnes[1], Kazuya Koyama[1], Misao Sasaki[2] and David Wands[1]
[1] *Institute of Cosmology and Gravitation, Mercantile House, University of Portsmouth, Portsmouth PO1 2EG, United Kingdom*
and
[2] *Yukawa Institute for Theoretical Physics, Kyoto University, Kyoto 606-8503, Japan*

We present Feynman type diagrams for calculating the n-point function of the primordial curvature perturbation in terms of scalar field perturbations during inflation. The diagrams can be used to evaluate the corresponding terms in the n-point function at tree level or any required loop level. Rules are presented for drawing the diagrams and writing down the corresponding terms in real space and Fourier space. We show that vertices can be renormalised to automatically account for diagrams with dressed vertices. We apply these rules to calculate the primordial power spectrum up to two loops, the bispectrum including loop corrections, and the trispectrum.

PACS numbers: 98.80.Cq YITP-07-30

I. INTRODUCTION

There is currently a great deal of interest in the statistical properties of primordial perturbations from inflation, because measurements of any non-Gaussianity will improve by about an order of magnitude over the next few years, for example with the Atacama Cosmology Telescope [1] and Planck [2]. This will provide a key way to discriminate between the many models of inflation. Although single field models of slow-roll inflation typically generate a small level of non-Gaussianity [3, 4], there may be an observable level generated in multiple field inflation [5], for example the curvaton scenario [6], or some single field models such as Dirac-Born-Infeld inflation (DBI) [7]. Currently observations of the CMB have concentrated on constraining the 3-point function (bispectrum) [8, 9, 10], but the 4-point function (trispectrum) has also been considered [11, 12, 13], and in principle higher order n-point functions may also be observable if they are sufficiently large. In some models the first signal of non-Gaussianity may come through the trispectrum, for example some special cases of the curvaton scenario [14]. Furthermore higher order statistics in principle carry more information and therefore could distinguish between different sources of non-Gaussianity, for example in many cases the bispectrum can be paremetrised by a single non-linearity parameter, f_{NL}, while the trispectrum depends on two wavenumber independent parameters, τ_{NL} and g_{NL} [14].

We will calculate the primordial curvature perturbation on uniform density hypersurfaces, ζ, on large scales employing the δN formalism [15, 16, 17, 18]. We use the separate universe approach [19, 20, 21]. This considers each super-Hubble scale patch to be evolving like a separate Friedmann-Robertson-Walker universe which are locally homogeneous. By patching these regions together we can track the evolution of the perturbations on large scales just by using background quantities which greatly simplifies our calculations. We also need to know the perturbations of the scalar fields at Hubble-exit, but in many cases these are extremely close to Gaussian in which case their statistical properties are given purely in terms of the power spectrum of the fields.

The number of e-foldings, N, given by

$$N = \int_{t_{\rm ini}}^{t_{\rm fin}} H(t) dt \,, \tag{1}$$

is evaluated from an initial flat hypersurface to a final uniform-density hypersurface. The perturbation in the number of e-foldings, δN, is the difference between the curvature perturbations on the initial and final hypersurfaces. We wish to calculate primordial perturbations, hence we pick a final uniform density hypersurface to be at a fixed time during the standard radiation dominated era, for example during primordial nucleosynthesis. The initial time is arbitrary provided it is after the Hubble exit time of all relevant scales. It is often convenient to pick this time to be shortly after Hubble-exit. We introduce the method for calculating the primordial curvature perturbation in terms of the δN formalism in more detail below.

Here we present a Feynman diagram type approach to calculating the primordial non-Gaussianity, where every term in the n-point function of ζ has a diagrammatic representation. Similar diagrams were introduced in the context of non-linear perturbation theory of large scale structure [22] and further developed in [23] (see also [24]). It is possible to read off the corresponding mathematical term in the n-point function for every diagram and it is possible to draw all the diagrams in a systematic way so that all terms are included. This approach extends to loop

corrections of any required order. Although the loop corrections are expected to be small in general compared to the tree level terms there is no proof of this, except for a particular loop correction to the bispectrum in some specific models of inflation [24]. We will see that in general the loop corrections depend on a large scale cut off; depending on this cut off the loop correction may contribute significantly to observable quantities, see for example [25, 26]. In fact there is a specific model of inflation where the one loop term gives the dominant and potentially observable contribution to the bispectrum [27]. A diagrammatic method to calculate field fluctuations during inflation was presented in [28].

We first introduce the primordial curvature perturbation. In the next two sections of this paper we assume the initial field perturbations are Gaussian, which in many cases is a good approximation to make, for example slow-roll inflation. In Sec. III A the rules for drawing diagrams in real space are given, along with a discussion of why we want to calculate connected rather than disconnected diagrams. In Sec. III B the equivalent rules in Fourier space are given. An application of the Fourier space rules for the power spectrum including second order loop corrections is given in Sec. III C. In Sec. IV we discuss a way to renormalise the vertices of the diagrams such that all diagrams with dressed vertices can be absorbed, with a proof given in the appendix. In Sec. V the assumption of Gaussian initial fields is dropped and the complete rules presented and applied to several examples. Finally we conclude in Sec. VI.

II. THE PRIMORDIAL CURVATURE PERTURBATION

We can write the primordial curvature perturbation, ζ, in terms of derivatives of N with respect to the fields, $N_A = \partial N/\partial\phi^A$ and the field perturbation, φ^A, at the initial time $t_{\rm ini}$. By neglecting any additional dependence on $\dot\phi^A$ at Hubble-exit we are assuming the field perturbations on large scales are overdamped and thus we can neglect the decaying mode. This is valid during slow roll, but also more generally holds for light fields during inflation. The assumption that N is a function of field values only is also valid in DBI inflation [29]. We use the notation that the fields are $\phi^A = \phi_0^A + \varphi^A$, where the perturbed field $\varphi^A \equiv \delta\phi^A$ satisfies $\langle\varphi^A\rangle = 0$. The curvature perturbation is given by

$$\zeta = \delta N - \langle\delta N\rangle = N_A\varphi^A + \frac{1}{2}N_{AB}\left(\varphi^A\varphi^B - \langle\varphi^A\varphi^B\rangle\right) + \frac{1}{3!}N_{ABC}\left(\varphi^A\varphi^B\varphi^C - \langle\varphi^A\varphi^B\varphi^C\rangle\right) + \cdots , \tag{2}$$

$$\text{where} \qquad \delta N = N_A\varphi^A + \frac{1}{2}N_{AB}\varphi^A\varphi^B + \frac{1}{3!}N_{ABC}\varphi^A\varphi^B\varphi^C + \cdots . \tag{3}$$

The dummy index A labels the light scalar fields relevant during inflation, and summation convention is used throughout this paper. It is more convenient to work with the ζ defined above since it satisfies $\langle\zeta\rangle = 0$, even though often $\zeta = \delta N$ is used in the literature. This equation can hence be used to calculate the primordial n-point function of ζ, although the result will depend on the n-point function of the fields at Hubble exit. This has so far been explicitly calculated for the 2-, 3- and 4-point functions, [4, 30, 31].

The connected 2-, 3- and 4-point functions of the fields are defined by

$$\langle\varphi^A_{\mathbf{k_1}}\,\varphi^B_{\mathbf{k_2}}\rangle = C^{AB}(k)(2\pi)^3\delta^3(\mathbf{k_1}+\mathbf{k_2}) , \tag{4}$$

$$\langle\varphi^A_{\mathbf{k_1}}\,\varphi^B_{\mathbf{k_2}}\,\varphi^C_{\mathbf{k_3}}\rangle = B^{ABC}(k_1,k_2,k_3)(2\pi)^3\delta^3(\mathbf{k_1}+\mathbf{k_2}+\mathbf{k_3}) , \tag{5}$$

$$\langle\varphi^A_{\mathbf{k_1}}\,\varphi^B_{\mathbf{k_2}}\,\varphi^C_{\mathbf{k_3}}\,\varphi^D_{\mathbf{k_4}}\rangle_c = T^{ABCD}(\mathbf{k}_1,\mathbf{k}_2,\mathbf{k}_3,\mathbf{k}_4)(2\pi)^3\delta^3(\mathbf{k_1}+\mathbf{k_2}+\mathbf{k_3}+\mathbf{k_4}) . \tag{6}$$

Note that only the 4-point function (and higher) depend on the direction of the $\mathbf{k}$ vectors, the 2- and 3-point functions of the fields just depend on the magnitude of the vectors, $k_i = |\mathbf{k}_i|$. Homogeneity of the random fields implies that the sum of the $\mathbf{k}$ vectors must be zero, while isotropy implies that the n-point functions are invariant under reorientations of this closed configuration.

At lowest order in slow roll different fields are uncorrelated at Hubble exit and all light fields have the same power spectrum [32, 33], so

$$C^{AB}(k) = \delta^{AB}P(k) , \tag{7}$$

where δ^{AB} is the Kronecker delta-function, and the variance per logarithmic interval in k-space is given by

$$\mathcal{P}(k) = \frac{4\pi k^3}{(2\pi)^3}P(k) = \left(\frac{H_*}{2\pi}\right)^2 , \tag{8}$$

where the Hubble parameter H is evaluated at Hubble-exit, $k = (aH)_*$. At zeroth order in slow-roll parameters, $\mathcal{P}$ is independent of wavenumber, i.e. we have a scale invariant spectrum for the field fluctuations. The bispectrum

satisfies $B^{ABC} = \mathcal{O}(\epsilon^{1/2}P^2)$ [30], where ϵ is a slow-roll parameter, so it is zero at lowest order in slow roll. However the trispectrum is not zero at lowest order in slow roll [31], $T^{ABCD} = \mathcal{O}(P^3)$, but is suppressed by $\mathcal{O}(P^2)$ compared to the power spectrum. For a discussion of the slow-roll order of higher order n-point functions of the fields see [34].

III. DIAGRAMS FOR GAUSSIAN FIELD PERTURBATIONS

Initially we will assume that all of the fields have a purely Gaussian distribution at an initial time, e.g. shortly after Hubble exit. Then every odd n-point function of the fields is zero and every even n-point function of the fields can be reduced to a product of 2-point functions. This assumption is not required and the extension to non-Gaussian field perturbations will be presented in Sec. V. However the approximation of initially Gaussian field perturbations is frequently made in the literature and is often a good approximation, for example [35] shows that the 3-point function of the fields adds an unobservably small contribution to the bispectrum around Hubble exit assuming slow roll inflation with a standard kinetic term of the scalar fields, while [31] show that the 4-point function of the fields adds an unobservably small contribution to the trispectrum around Hubble exit under the same assumptions.

Working to zeroth order in slow roll implies that (7) holds and that the 3-point function of the fields is zero. So although working to lowest order in slow roll is not the same as working with Gaussian field perturbations, in practice the conditions are related. Hence when assuming that the field perturbations have a Gaussian distribution at Hubble exit we will also work at zeroth order in slow roll. It is likely that any observable amount of non-Gaussianity can be calculated to sufficiently high accuracy when making these two approximations, assuming a standard kinetic term.

A. Real space diagrams

Assuming that the fields are uncorrelated Gaussian variables, with identical distributions, as discussed above, the two point function of the fields is given by

$$\langle \varphi^A_{x_i} \varphi^B_{x_j} \rangle = \begin{cases} \delta^{AB} G(|x_i - x_j|) & \text{for } i \neq j, \\ \delta^{AB} \langle \varphi^2 \rangle & \text{for } i = j. \end{cases} \tag{9}$$

All of the higher n-point functions of the fields can be written in terms of G and the variance of the fields $\langle \varphi^2 \rangle$. The two point function G only depends on $|x_i - x_j|$ because we are assuming the background is homogenous and isotropic.

The diagrammatic rules for the connected n-point function, $\langle \zeta_{x_1} \zeta_{x_2} \cdots \zeta_{x_n} \rangle_c$, are:

1. Draw n points representing the n spatial points $x_1, \cdots, x_n$ and connect them with r propagators (dashed lines) which attach two of the positions x_i (it can be two distinct positions or it can have both ends attached to the same position). The diagram should be connected in order to calculate the connected n point function, see Sec. III A 1. We require $r \geq n-1$ in order to draw a connected diagram and diagrams with $r = n-1$ are tree level, while those with $r > n-1$ include loop corrections.

2. Label each end of each propagator with the field indices $A, B, \ldots C$.

3. Assign a factor $N_{AB\cdots C}$ to each spatial point, x_i, where the number of derivatives of N is the number of propagators attached to that x_i.

4. Assign a factor of $\delta^{AB} G(|x_i - x_j|)$ to each propagator, where AB are the appropriate field indices attached to the propagator and x_i, x_j are the positions at either end of the propagator. If both ends of the propagator are attached to the same x_i instead assign a factor $\delta^{AB}\langle \varphi^2 \rangle$.

5. Divide by the appropriate numerical factor. Whenever l propagators attach the same x_i and x_j at both ends this gives a factor of $l!$. Whenever l propagators dress an x_i this gives an additional factor of 2^l (as well as the factor of $l!$ due to the previous rule). A propagator dresses an x_i if both ends of the propagator are attached to the same x_i.

6. Add all permutations of the diagrams which is all of the distinct ways to relabel the spatial points. The number of permutations depends on the symmetries of the diagram, a diagram with complete symmetry between all of the spatial points has only one term, while for a diagram with no symmetries between the spatial points there are $n!$ permutations.

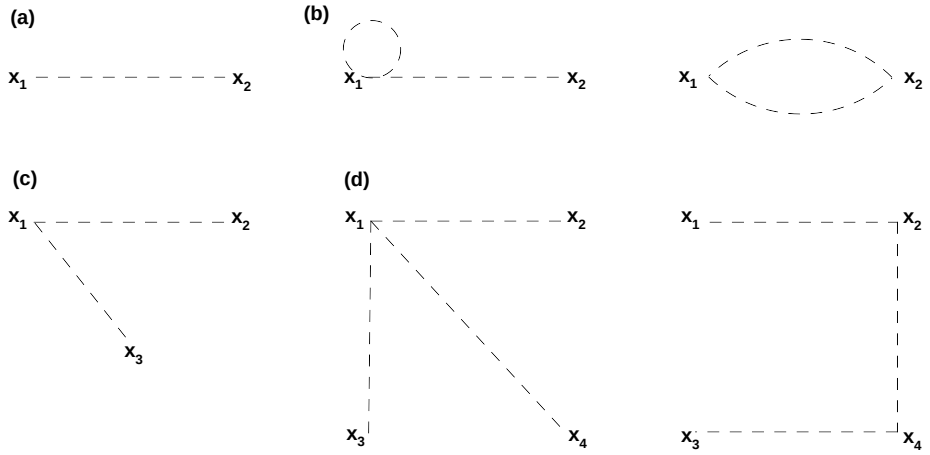

FIG. 1: The 2-point function at tree (a) and one loop level (b), and the 3- and 4-point functions at tree level, (c) and (d) respectively. All figures in this paper were drawn using JaxoDraw [36].

In Fig. 1 the diagrams for the 2-point function at tree level and one loop level, plus the tree level terms for the 3- and 4-point functions are shown. Note that for the 4-point function there are two tree level terms.

The terms corresponding to the diagrams are given below, in the same order as the diagrams,

$$\langle\zeta_{x_1}\zeta_{x_2}\rangle = \left(N_A N^A + N_A N_B^{AB}\langle\varphi^2\rangle\right) G(|x_1-x_2|) + \frac{1}{2}N_{AB}N^{AB}G(|x_1-x_2|)^2\,, \tag{10}$$

$$\langle\zeta_{x_1}\zeta_{x_2}\zeta_{x_3}\rangle = N_A N_B N^{AB}\left(G(|x_1-x_2|)G(|x_1-x_3|) + 2\text{ perms}\right)\,, \tag{11}$$

$$\begin{aligned}\langle\zeta_{x_1}\zeta_{x_2}\zeta_{x_3}\zeta_{x_4}\rangle_c &= N_A N_B N_C N^{ABC}\left(G(|x_1-x_2|)G(|x_1-x_3|)G(|x_1-x_4|) + 3\text{ perms}\right)\\ &\quad + N_A N_B N_C^A N^{BC}\left(G(|x_1-x_2|)G(|x_2-x_3|)G(|x_3-x_4|) + 11\text{ perms}\right)\,.\end{aligned} \tag{12}$$

Although the second diagram for the two point function, Fig. 1, has a dressed vertex with an associated numerical factor of 2, there is another permutation of this diagram with the x_2 dressed which gives an equal contribution. The third diagram has two propagators attaching x_1 and x_2 and there are no other permutations of this diagram so there is a numerical factor of 2, as shown in the third term of (10). The diagrams for the 3- and 4-point functions are all at tree level so they all have a numerical factor of 1. The first diagram for the 4-point function has 4 permutations since we have 4 choices of which of the $x_1,\cdots,x_4$ has 3 propagators attached to it as given in the first term of (12), the second diagram of the 4-point function has 12 permutations because there are 4×3 choices of which 2 of the $x_1,\cdots,x_4$ should have 2 propagators attached to them

1. *Disconnected diagrams*

In general any n-point function has a connected and a disconnected part. Throughout this paper we will only consider the connected n-point function because the disconnected contribution contains no new information over the lower n-point functions that it is split into. There is no disconnected contribution to the 2- or 3-point function of the fields or zeta, because we assume $\langle\varphi^A\rangle = \langle\zeta\rangle = 0$. The disconnected contribution is only non-zero if a subset of the $\mathbf{k}$ vectors sums to zero.

For example the disconnected part of the primordial 4-point function, $\langle\zeta^A_{\mathbf{k}_1}\,\zeta^B_{\mathbf{k}_2}\,\zeta^C_{\mathbf{k}_3}\zeta^D_{\mathbf{k}_4}\rangle$, is the product of two 2-point functions such as $\langle\zeta^A_{\mathbf{k}_1}\,\zeta^B_{\mathbf{k}_2}\rangle\langle\zeta^C_{\mathbf{k}_3}\zeta^D_{\mathbf{k}_4}\rangle$ and in total there are three such terms. This is non-zero even if ζ is purely Gaussian, but it contains no new information compared to the primordial 2-point function. This term only contributes if $\mathbf{k}_i + \mathbf{k}_j = 0$ for some $i,j = 1,\cdots,4$, so provided the sum of any two $\mathbf{k}$ vectors is not zero any contribution is from the connected part. The connected part of the primordial 4-point function is only non-zero if ζ is not purely Gaussian and it contains information that is not observable from the primordial 2- or 3-point functions.

B. Fourier space diagrams

We present here the rules for drawing the connected diagrams (see Sec. III A 1) of the n-point function of ζ at r-th order (i.e. $\mathcal{O}(\mathcal{P}^r)$), for $r \geq n-1$. The tree level terms correspond to $r = n-1$.

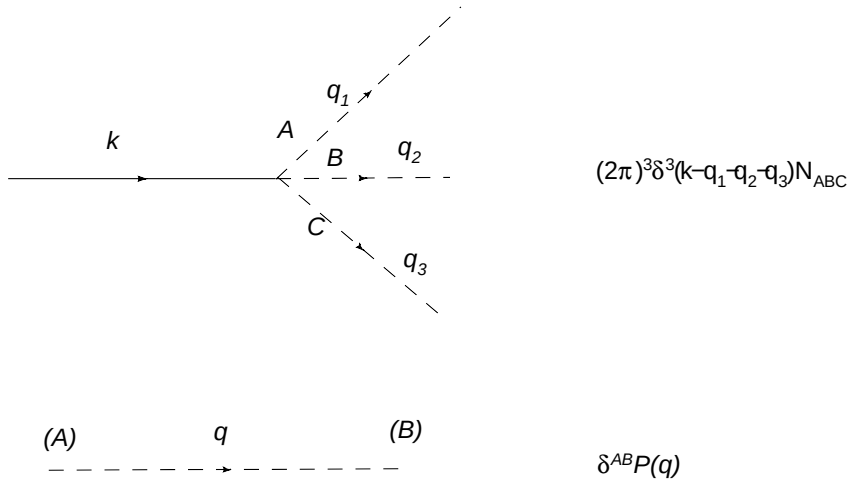

FIG. 2: The terms that are associated with every vertex and propagator.

1. Draw all distinct connected diagrams with n-external (solid) lines and r (dashed) propagators. Every vertex must consist of 1 external line and at least 1 propagator.

2. Label the external legs with incoming momenta $\mathbf{k}_i$ for $i = 1, \cdots, n$ and label the propagators with internal momenta $\mathbf{q}_i$ for $i = 1, \cdots, r$. Label each end of each propagator with a field index $A, B, \cdots, C$.

3. Assign a factor $N_{AB\cdots C}(2\pi)^3\delta^3(\mathbf{k_i} - \mathbf{q_1} - \cdots - \mathbf{q_p})$ to each vertex. The number of derivatives of N corresponds to the number of propagators attached to each vertex. We use the convention that incoming momentum is positive. The δ function ensures momentum is conserved at each vertex. See Fig. 2.

4. Assign a factor $\delta^{AB}P(q)$ to each propagator, where AB are the appropriate field indices that the propagator is labelled with at either vertex and $\mathbf{q}$ is the momentum attached to the propagator. See Fig. 2.

5. Integrate over the propagator momenta, $\frac{1}{(2\pi)^3}\int d^3q_i$. The first $n-1$ integrations are trivial because of the δ functions but any further integrations (in the case of a diagram with loop corrections) cannot in general be evaluated analytically.

6. Divide by the appropriate numerical factor. Whenever l propagators attach the same vertices at both ends this gives a factor of $l!$. Whenever l propagators dress a vertex this gives an additional factor of 2^l (as well as the factor of $l!$ due to the previous rule). A propagator dresses a vertex if both ends of the propagator are attached to the same vertex.

7. Add all permutations of the diagrams which is all of the distinct ways to relabel the $\mathbf{k}_i$ attached to the external lines. The number of permutations depends on the symmetries of the diagram, a diagram with complete symmetry between all of the external lines has only one term, while for a diagram with no symmetries between the external lines there are $n!$ permutations.

1. Comments on the diagrams and their rules

Going between the unlabelled diagrams in Fourier or real space is straightforward, to go from Fourier space to real space one simply removes the external lines and places an x_i at each vertex. To go from real space to Fourier space one attaches an external line in place of every x_i.

In Fourier space rule 1 for the diagram is to draw every possible diagram at the appropriate order. Rule 2 gives the rules for labelling the diagrams. Rules 3–5 give the associated mathematical expression for each diagram, up to a numerical factor given in rule 6. A derivation of the numerical factors is given in Sec. IV and App. A 1. The numerical factor for all tree level diagrams is 1. Finally rule 7 tells one to include every permutation of the labelling of the $\mathbf{k}_i$ on the external legs that are distinct.

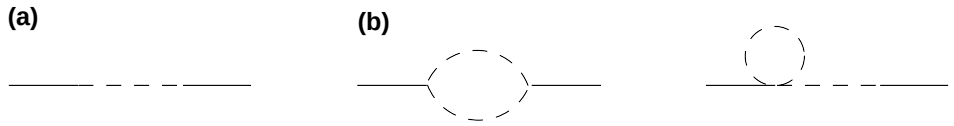

FIG. 3: The tree level (a) and 1 loop correction (b) for the power spectrum.

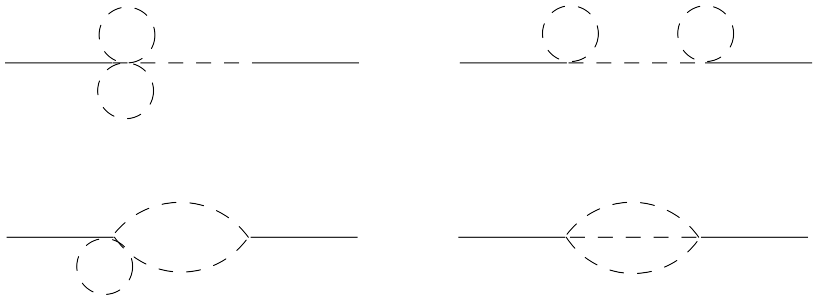

FIG. 4: The two loop terms for the power spectrum with a Gaussian initial field.

C. Power spectrum

The primordial power spectrum in Fourier space is defined by

$$\langle \zeta_{\mathbf{k}_1} \zeta_{\mathbf{k}_2} \rangle \equiv P_\zeta(k) (2\pi)^3 \delta^3(\mathbf{k_1} + \mathbf{k_2}) \,. \tag{13}$$

The tree level and one loop correction terms to the 2-point function is diagrammatically given by Fig. 3. After carrying out the trivial integration over the propagator momentum the tree level term is given by

$$P_\zeta^{\rm tree}(k) = N_A N^A P(k) \,. \tag{14}$$

The one loop terms are given by

$$P_\zeta^{1\ {\rm loop}}(k) = \frac{1}{(2\pi)^3} \int d^3q \left(\frac{1}{2} N_{AB} N^{AB} P(q) P(|\mathbf{k}_1 - \mathbf{q}|) + N_A N_B^{AB} P(k) P(q) \right) , \tag{15}$$

where we have already carried out one integration. Both of the diagrams associated with these terms have a numerical factor of 2, however there are also 2 permutations of the second term because it has a non symmetric diagram. Because of momentum conservation, $\mathbf{k}_1 + \mathbf{k}_2 = 0$, it follows that $k_1 = k_2$. After enforcing $k \equiv k_1 = k_2$ the two permutations of the second diagram give an equal contribution which cancels the numerical factor of 2.

Going to 2 loops, terms of order $\mathcal{P}^3$ there are four terms. Diagrammatically the terms are given in Fig. 4 which corresponds to

$$\begin{aligned} P_\zeta^{2\ {\rm loop}} \;=\; & \frac{1}{(2\pi)^6} \int d^3q_1 d^3q_2 \left(\frac{1}{4} N_{ABC}^{AB} N^C P(q_1) P(q_2) P(k) + \frac{1}{4} N_{AB}^A N_C^{BC} P(k) P(q_1) P(q_2) \right. \\ & \left. + \frac{1}{2} N_{AB} N_C^{ABC} P(q_1) P(q_2) P(|\mathbf{k}_1 - \mathbf{q}_2|) + \frac{1}{6} N_{ABC} N^{ABC} P(q_1) P(|\mathbf{q}_2 - \mathbf{q}_1|) P(|\mathbf{k}_1 - \mathbf{q}_2|) \right) . \end{aligned} \tag{16}$$

Only the fourth diagram of Fig. 4 does not have a dressed vertex. In fact at every level there is only one diagram without dressed vertices, as has already been shown explicitly at tree and one loop level in Fig. 3.

D. Evaluation of the 1 loop diagrams

In the case where a single field ϕ generates the primordial curvature perturbation, so $N = N(\phi)$, we have

$$P_\zeta^{\rm tree}(k) = (N')^2 P(k) \,, \tag{17}$$

where $N' = \partial N / \partial \phi$. In the case of a scale invariant spectrum we can also evaluate the 1 loop integrals if we apply a large scale cut off L. For a discussion of how to evaluate the integral over the loop momenta and the dependence

of this term on the cut off L see for example [37]. We also apply a small scale cut off k. The result is

$$P_\zeta^{1\ \mathrm{loop}}(k) = P(k)\mathcal{P}\left((N'')^2 + N'''N'\right)\log(kL)\,, \tag{18}$$

where the variance $\mathcal{P}$ was defined by Eq. (8). In analogy with Eq. (8) we define $\mathcal{P}_\zeta = P_\zeta(k)k^3/(2\pi^2)$ which from observations of the CMB is of the order 10^{-10} [38]. We hence have

$$\frac{P_\zeta^{1\ \mathrm{loop}}(k)}{P_\zeta^{\mathrm{tree}}(k)} = \mathcal{P}_\zeta^{\mathrm{tree}}\left(\frac{(N'')^2}{(N')^4} + \frac{N'''}{(N')^3}\right)\log(kL)\,. \tag{19}$$

We can write the derivatives of N in terms of the (in principle) observable non-linearity parameters f_{NL} and g_{NL} which in this case can be defined by [10, 39]

$$\zeta = \zeta_1 + \frac{3}{5}f_{NL}\zeta_1^2 + \frac{9}{25}g_{NL}\zeta_1^3 + \cdots\,, \tag{20}$$

where ζ_1 is Gaussian because it is directly proportional to the initial Gaussian field perturbation, φ_1, and the dimensionless non-linearity parameters, f_{NL} and g_{NL}, are given by

$$f_{NL} = \frac{5}{6}\frac{N''}{(N')^2}\,, \tag{21}$$

$$g_{NL} = \frac{25}{54}\frac{N'''}{(N')^3}\,. \tag{22}$$

For the extension of these two formula to the case of multiple field inflation see for example [14]. Substituting (21) and (22) into (19) we find

$$\frac{P_\zeta^{1\mathrm{loop}}(k)}{P_\zeta^{\mathrm{tree}}(k)} = \mathcal{P}_\zeta^{\mathrm{tree}}\left(\frac{36}{25}f_{NL}^2 + \frac{54}{25}g_{NL}\right)\log(kL)\,. \tag{23}$$

If $\mathcal{P}_\zeta^{\mathrm{tree}} \sim 10^{-10}$ and we take the large scale cut off to be comparable to the present day Hubble scale then we can take $\log(kL) = O(1)$ [27, 37], and the observational bound on the bispectrum, $|f_{NL}| \lesssim 100$ [38] bounds the first term of the ratio above to be less than 10^{-6}. There is not yet any equivalent observational bound on g_{NL} but it would have to be extremely large in order to give a significant contribution to Eq. (23). It therefore seems that the only way for the 1 loop contribution to be significant compared to the tree level term of the power spectrum is to take an exponentially large cut off L. For a discussion of this possibility see for example [25, 26].

IV. RENORMALISATION

There is a way to reduce the number of diagrams significantly, by renormalising the vertices such that the diagrams with dressed vertices are automatically accounted for. We do this by renormalising the factors $N_{AB\cdots C}$, that are attached to each vertex.

The derivative of the number of e-foldings for the given background ϕ_0 is $N_{AB\cdots C} \equiv N_{AB\cdots C}|_{\phi_0}$, and we can relate this to the number of e-foldings at a general point $\mathbf{x}$ by

$$\tilde{N} \equiv N(\phi(\mathbf{x})) = N|_{\phi_0} + N_A\varphi^A + \frac{1}{2}N_{AB}\varphi^A\varphi^B + \frac{1}{3!}N_{ABC}\varphi^A\varphi^B\varphi^C + \cdots\,. \tag{24}$$

The expectation of $\tilde{N}_{AB\cdots C}$ is given by

$$\langle\tilde{N}_{AB\cdots C}\rangle = N_{AB\cdots C} + \frac{1}{2}N^D_{AB\cdots CD}\langle\varphi^2\rangle + \frac{1}{8}N^{DE}_{AB\cdots CDE}\langle\varphi^2\rangle^2 + \cdots\,, \tag{25}$$

where we have used Wick's theorem to decompose the expectation of powers of φ according to

$$\langle\varphi^{2n}\rangle = (2n-1)!!\langle\varphi^2\rangle^n, \qquad \langle\varphi^{2n-1}\rangle = 0\,. \tag{26}$$

The double factorial is defined by $(2n-1)!! = (2n-1)(2n-3)\cdots 5\cdot 3\cdot 1$. The coefficient of the general term in (25), $\langle\varphi^2\rangle^n$ is given by (24) and (26) and is $(2n-1)!!/(2n)! = 1/(2^n n!)$. This explains the numerical factor associated with every dressed vertex, see rule 6, Sec. III B.

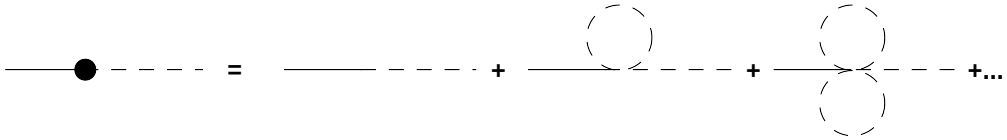

FIG. 5: Graphical representation of $\langle \tilde{N}_A \rangle$.

In Fourier space the ensemble average of $\tilde{N}_{AB\cdots C}$ is

$$\langle \tilde{N}_{AB\cdots C} \rangle = N_{AB\cdots C} + \frac{1}{2} N^D_{AB\cdots CD} \frac{1}{(2\pi)^3} \int d^3q P(q) + \frac{1}{8} N^{DE}_{AB\cdots CDE} \frac{1}{(2\pi)^6} \int d^3q_1 d^3q_2 P(q_1) P(|\mathbf{q}_2 - \mathbf{q}_1|) + \cdots , \quad (27)$$

which in real space is given by Eq. (25).

In Fig. 5 the graphical representation of $\langle \tilde{N}_A \rangle = N_A + \frac{1}{2} N^B_{AB} \langle \varphi^2 \rangle + \frac{1}{8} N^{BC}_{ABC} \langle \varphi^2 \rangle^2 + \cdots$ is given up to 2 loops. So far the derivatives of N had been calculated at ϕ_0, however if we instead calculate the expectation of the derivative of N at a general point, and attach this factor $\langle \tilde{N}_{AB\cdots C} \rangle$ to each vertex (which we call a renormalised vertex) then all diagrams with dressed vertices are automatically included in the expansion (25) and don't need to be drawn. We provide a proof of this in appendix A.

A. Renormalised real space diagrams

The new diagrammatic rules for the connected n-point function with renormalised vertices are:

1. Draw n points representing the n spatial points $x_1, \cdots, x_n$ and connect them with r propagators (dashed lines) which attach two distinct positions x_i and x_j. The vertices are drawn with a solid dot to show that they are renormalised, see Fig. 6 for examples of such diagrams. The diagram should be connected in order to calculate the connected n point function, see Sec. III A 1. We require $r \geq n-1$ in order to draw a connected diagram and diagrams with $r = n-1$ are tree level, while those with $r > n-1$ include loop corrections.

2. Label each end of each propagator with the field indices $A, B, \ldots C$.

3. Assign a factor $\langle \tilde{N}_{AB\cdots C} \rangle$ to each spatial point, x_i, where the number of derivatives of $\tilde{N}$ is the number of propagators attached to that x_i.

4. Assign a factor of $\delta^{AB} G(|x_i - x_j|)$ to each propagator, where AB are the appropriate field indices attached to the propagator and x_i, x_j are the positions at either end of the propagator.

5. Divide by the appropriate numerical factor. Whenever l propagators attach the same x_i and x_j at both ends this gives a factor of $l!$.

6. Add all permutations of the diagrams which is all of the distinct ways to relabel the spatial points. The number of permutations depends on the symmetries of the diagram, a diagram with complete symmetry between all of the spatial points has only one term, while for a diagram with no symmetries between the spatial points there are $n!$ permutations.

In Fig. 6 the diagrams for the 2-point function up to two loop level is presented.
The terms corresponding to the diagrams are given below, in the same order as the diagrams,

$$\begin{aligned} \langle \zeta_{x_1} \zeta_{x_2} \rangle \;=\; & \langle \tilde{N}_A \rangle \langle \tilde{N}^A \rangle G(|x_1 - x_2|) + \frac{1}{2} \langle \tilde{N}_{AB} \rangle \langle \tilde{N}^{AB} \rangle G(|x_1 - x_2|)^2 \\ & + \frac{1}{3!} \langle \tilde{N}_{ABC} \rangle \langle \tilde{N}^{ABC} \rangle G(|x_1 - x_2|)^3 + \cdots . \end{aligned} \quad (28)$$

Note that with the renormalised diagrams there is only one diagram at every order in loops. This result is also derived to all orders in App. A.

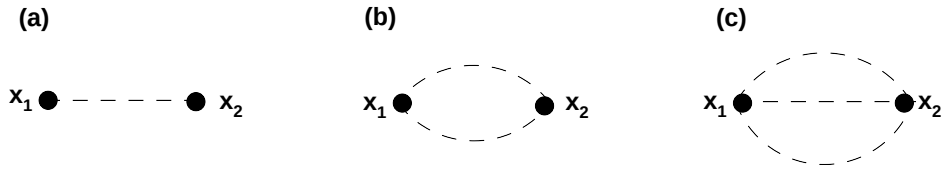

FIG. 6: The 2-point function at tree, 1 loop and 2 loop levels ((a), (b) and (c) respectively), with renormalised propagators.

FIG. 7: The power spectrum at tree, (a), 1, (b), and 2, (c), loop levels with renormalised propagators.

B. Renormalised Fourier space diagrams

Rules for drawing the connected diagrams (see Sec. III A 1) of the n-point function of ζ at r-th order (i.e. $\mathcal{O}(\mathcal{P}^r)$), for $r \geq n-1$. The tree level terms correspond to $r = n-1$.

1. Draw all distinct connected diagrams with n external (solid) lines and r (dashed) propagators. Every renormalised vertex must consist of 1 external line and at least 1 propagator, and drawn with a solid dot to show that the vertex is renormalised. The propagators cannot have both ends attached to the same vertex.

2. Label the external legs with incoming momenta $\mathbf{k}_i$ for $i = 1, \cdots, n$ and label the propagators with internal momenta $\mathbf{q}_i$ for $i = 1, \cdots, r$. Label each end of each propagator with a field index $A, B, \cdots, C$.

3. Assign a factor $\langle \tilde{N}_{AB\cdots C} \rangle \delta^3(\mathbf{k_i} - \mathbf{q_1} - \cdots - \mathbf{q_p})$ to each vertex. The number of derivatives of $\tilde{N}$ corresponds to the number of propagators attached to each vertex. We use the convention that incoming momentum is positive. The δ function ensures momentum is conserved at each vertex.

4. Assign a factor $\delta^{AB} P(q)$ to each propagator, where AB are the appropriate field indices that the propagator is labelled with at either vertex and $\mathbf{q}$ is the momentum attached to the propagator.

5. Integrate over the propagator momenta, $\frac{1}{(2\pi)^3} \int d^3 q_i$. The first $n-1$ integrations are trivial because of the δ functions but any further integrations (in the case of a diagram with loop corrections) cannot in general be evaluated analytically.

6. Divide by the appropriate numerical factor. Whenever l propagators attach the same vertices at both ends this gives a factor of $l!$.

7. Add all permutations of the diagrams which is all of the distinct ways to relabel the $\mathbf{k}_i$ attached to the external lines. The number of permutations depends on the symmetries of the diagram, a diagram with complete symmetry between all of the external lines has only one term, while for a diagram with no symmetries between the external lines there are $n!$ permutations.

C. Power spectrum

We again calculate the power spectrum up to 2 loop level, this time with renormalised vertices. There is only one diagram at every loop level, we present the three lowest order diagrams in Fig. 7, which correspond to

$$\begin{aligned} P_\zeta^{\text{up to 2 loop}} &= \langle \tilde{N}_A \rangle \langle \tilde{N}^A \rangle P(k) + \frac{1}{2} \frac{1}{(2\pi)^3} \int d^3 q \langle \tilde{N}_{AB} \rangle \langle \tilde{N}^{AB} \rangle P(q) P(|\mathbf{k}_1 - \mathbf{q}|) \\ &\quad + \frac{1}{3!} \frac{1}{(2\pi)^6} \int d^3 q_1 d^3 q_2 \langle \tilde{N}_{ABC} \rangle \langle \tilde{N}^{ABC} \rangle P(q_1) P(|\mathbf{q}_2 - \mathbf{q}_1|) P(|\mathbf{q}_2 - \mathbf{k}_1|) \,. \end{aligned} \tag{29}$$

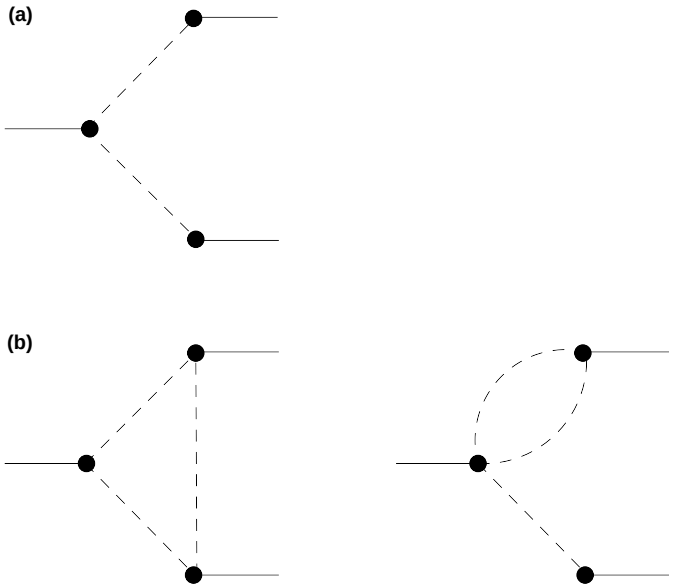

FIG. 8: The bispectrum at tree, (a), and 1 loop, (b), levels, with renormalised propagators.

D. Bispectrum

We calculate the bispectrum including the leading order loop corrections. The bispectrum is defined by

$$\langle \zeta_{\mathbf{k}_1}\, \zeta_{\mathbf{k}_2}\, \zeta_{\mathbf{k}_3} \rangle \equiv B_\zeta(k_1, k_2, k_3)(2\pi)^3 \delta^3(\mathbf{k_1} + \mathbf{k_2} + \mathbf{k_3})\,. \tag{30}$$

At tree level there is one term and at 1 loop level there are two terms, which are shown diagrammatically by Fig. 8 and these give the contribution

$$B_\zeta^{\rm tree} = \langle \tilde{N}_{AB}\rangle \langle \tilde{N}^A\rangle \langle \tilde{N}^B\rangle \left(P(k_1)P(k_2) + 2 \text{ perms}\right)\,, \tag{31}$$

$$\begin{aligned} B_\zeta^{1\text{ loop}} = \frac{1}{(2\pi)^3}\int d^3q \Big(& \langle \tilde{N}_{AB}\rangle \langle \tilde{N}^A_C\rangle \langle \tilde{N}^{BC}\rangle P(q)P(|\mathbf{k}_1 - \mathbf{q}|)P(|\mathbf{k}_2 + \mathbf{q}|) \\ & + \frac{1}{2}\langle \tilde{N}_{ABC}\rangle \langle \tilde{N}^A\rangle \langle \tilde{N}^{BC}\rangle \left(P(k_1)P(q)P(|\mathbf{k}_2 - \mathbf{q}|) + 5 \text{ perms}\right) \Big)\,. \end{aligned} \tag{32}$$

V. EXTENSION TO NON-GAUSSIAN FIELDS IN FOURIER SPACE

If we don't assume that the scalar fields are Gaussian at the initial time (e.g. Hubble exit) we have to take account of the higher n-point functions of the fields. This is likely to be important in models with a non-standard kinetic term where the non-Gaussianity of the fields may be large at Hubble exit [40], for example DBI inflation inspired from brane world models, [7, 29]. The connected 2-, 3- and 4-point function of the fields are defined in (4)–(6).

Our analysis relies on the δN-formalism which assumes that N is a function of the field values ϕ^A but not the field derivatives independently as well. However we can still go beyond leading order in a slow-roll expansion and derive expressions which are valid to arbitrary order in slow roll, for example the different fields are in general correlated at Hubble exit, at first order in slow roll, see [32, 33].

1. *Extended rules for the diagrams with non-Gaussian fields*

The diagrams are more complicated since while the 2-point function is still drawn as a propagator the higher n-point functions are drawn by an n-point vertex of dashed lines.

The rules for the diagrams are now:

1. Draw all distinct connected diagrams with n-external (solid) lines and the appropriate number of internal correlators, which can be propagators (2-point functions) or higher n-point correlators of the fields. The order of the connected n-point function of the field perturbations is $n-1$, i.e. $\langle\varphi^n\rangle_c \sim \mathcal{O}(\mathcal{P}^{n-1})$. There cannot be more than one external line attached to each vertex. Every dashed line must be attached to an external line on at least one end, if it is attached to an external line on both ends it is a propagator (a correlator of order 2).

2. Label the external lines with incoming momenta $\mathbf{k}_i$ for $i = 1, \cdots, n$ and label each dashed line with internal momenta $\mathbf{q}_i$ for $i = 1, \cdots, r$. Label each dashed line at a vertex containing an external line with a field index $A, B, \cdots C$.

3. Assign a factor $N_{AB\cdots C}(2\pi)^3\delta^3(\mathbf{k} - \mathbf{q_1} - \cdots - \mathbf{q_p})$ to each vertex which includes an external line, where the number of derivatives of N corresponds to the number of dashed lines attached to that vertex. The δ function ensures momentum is conserved at each vertex. See Fig. 9.

4. Assign a factor $C^{AB}(q)$ to each propagator, where AB are the appropriate field indices that the propagator is labelled with at either vertex and $\mathbf{q}$ is the momentum attached to the propagator. See Fig. 9.

5. Assign a factor $(2\pi)^3\delta^3(\mathbf{q_1} + \mathbf{q_2} + \mathbf{q_3})B^{ABC}(q_1, q_2, q_3)$ to each vertex of three dashed lines and no external lines (which corresponds to a 3-point function of the fields), where A, B and C are the field indices attached to the dashed lines where they meet a vertex with an external line. See Fig. 9 again. Similar rules hold for vertices of dashed lines at higher order.

6. Integrate over all internal momenta, $\frac{1}{(2\pi)^3}\int d^3q_i$. For a tree diagram all of the integrations are trivial, but in the case of a diagram with loop corrections there will be some integrals which in general cannot be evaluated analytically.

7. Divide by the appropriate numerical factor. Whenever l propagators or higher order correlators of the fields attach the same vertices (and with the same number of lines to each vertex) at both ends this gives a factor of $l!$. If u legs from a higher order correlator are attached to the same vertex this gives an extra factor of $u!$. It follows that if l correlators, each of order p, all dress the same vertex then this gives a numerical factor of $l!(p!)^l$. See App. A 2 for a proof of these rules and see Fig. 13 for two example of dressed vertices, the associated terms with the numerical factors are given in (A21), (A22).

8. Add all permutations of the diagrams which is all of the distinct ways to relabel the $\mathbf{k}_i$ attached to the external lines. The number of permutations depends on the symmetries of the diagram, a diagram with complete symmetry between all of the external lines has only one term, while for a diagram with no symmetries between the external lines there are $n!$ permutations.

A. Power spectrum

We give again the power spectrum defined by (13), but this time for non-Gaussian initial fields and valid to all orders in slow roll. There is one extra diagram at one loop level, and six extra diagrams at two loop level. Because of momentum conservation, $\mathbf{k}_1 + \mathbf{k}_2 = 0$, it follows that $k_1 = k_2 \equiv k$. Therefore even the non-symmetric diagrams which would have two permutations only correspond to a single term after enforcing this symmetry.

The tree level term is given by

$$P_\zeta^{\rm tree}(k) = N_A N_B C^{AB}(k)\,, \tag{33}$$

notice that at leading order in slow roll using (7) this reduces to (14).

The one loop terms are given by

$$\begin{aligned} P_\zeta^{1\ \rm loop}(k) \;=\; & \frac{1}{(2\pi)^3}\int d^3q \Big(\frac{1}{2}N_{AB}N_{CD}C^{AC}(q)C^{BD}(|\mathbf{k}_1 - \mathbf{q}|) + N_A N_{BCD}C^{AB}(k)C^{CD}(q) \\ & + N_A N_{BC}B^{ABC}(k, q, |\mathbf{k}_1 - \mathbf{q}|)\Big)\,, \end{aligned} \tag{34}$$

where the extra one loop term which does not appear for Gaussian fields is shown in Fig. 10, and the first two terms were shown diagrammatically in Fig. 4. Going to 2 loops, terms of order $\mathcal{P}^3$ there are ten terms, only the last four

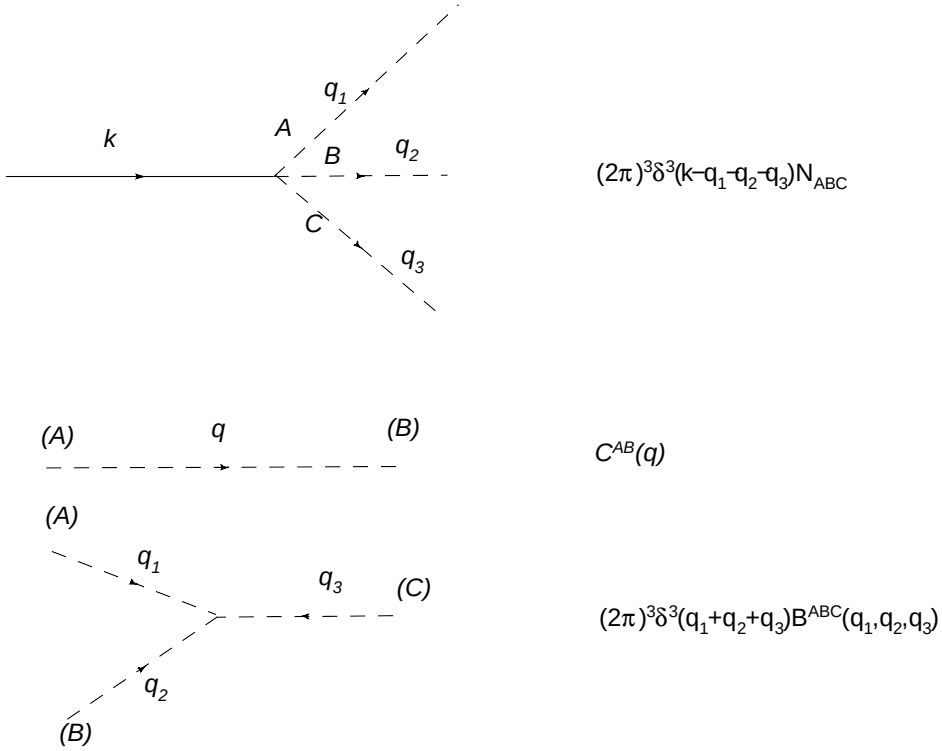

FIG. 9: The terms that are associated with every vertex, propagator and higher order correlator.

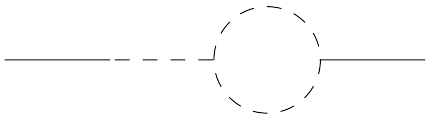

FIG. 10: The extra one loop term for the power spectrum with a non-Gaussian field.

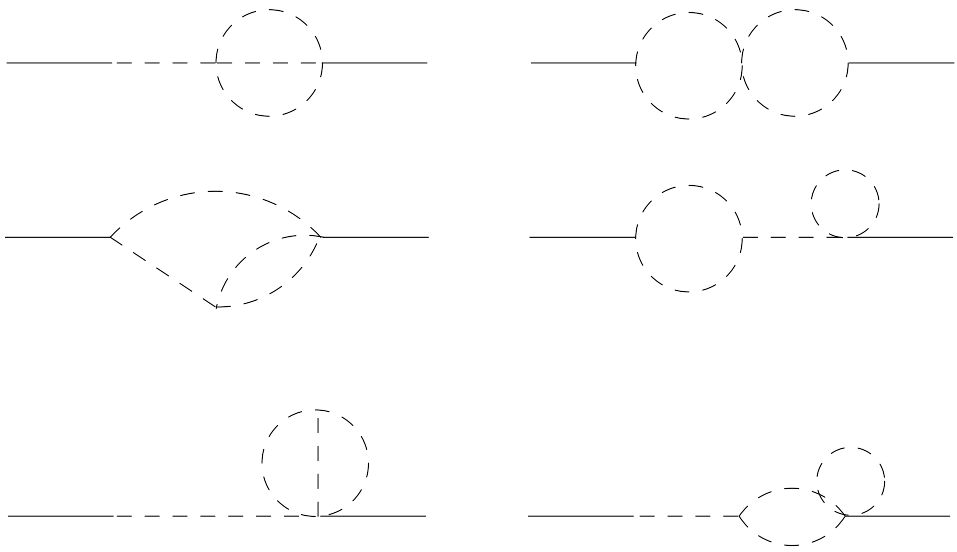

FIG. 11: The two loop terms for the power spectrum which involve a 4-point function of the fields.

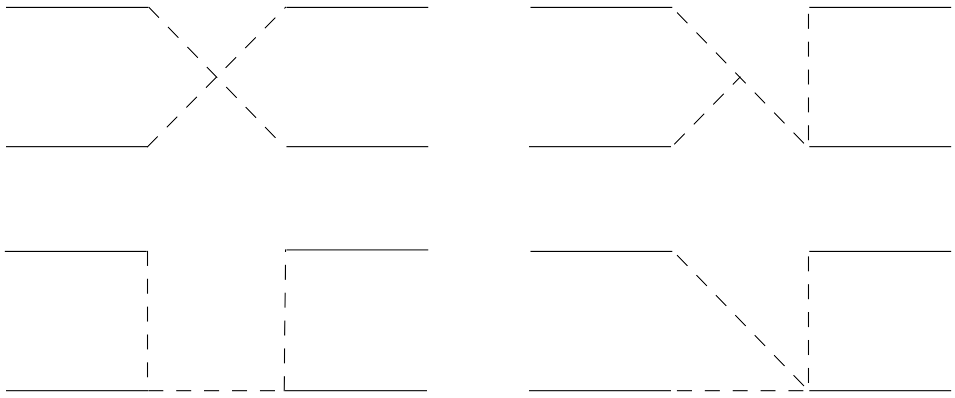

FIG. 12: Tree level terms of the 4-point function.

of which are non-zero for a Gaussian field. Diagrammatically the terms involving a 3-point or 4-point function of the fields are given in Fig. 11, which corresponds to the first six terms of

$$\begin{aligned}
P_\zeta^{2\text{ loop}} \;=\; & \frac{1}{(2\pi)^6}\int d^3q_1 d^3q_2 \left(\frac{1}{3}N_A N_{BCD} T^{ABCD}(\mathbf{q}_1, \mathbf{q}_2-\mathbf{q}_1, \mathbf{k}_1-\mathbf{q}_2, \mathbf{k}_2)\right. \\
& +\frac{1}{4}N_{AB}N_{CD}T^{ABCD}(\mathbf{q}_1, \mathbf{k}_1-\mathbf{q}_1, \mathbf{q}_2, \mathbf{k}_2-\mathbf{q}_2) \\
& +N_{AB}N_{CDE}B^{BDE}(|\mathbf{k}_1+\mathbf{q}_1|, |\mathbf{q}_2-\mathbf{q}_1|, |\mathbf{k}_2-\mathbf{q}_2|)C^{AC}(q_1)+\frac{1}{2}N_{AB}N_{CDE}B^{ABC}(k, q_1, |\mathbf{k}_2+\mathbf{q}_1|)C^{DE}(q_2) \\
& +\frac{1}{3}N_A N_{BCDE}B^{CDE}(q_1, |\mathbf{q}_1+\mathbf{q}_2|, q_2)C^{AB}(k)+\frac{1}{2}N_A N_{BCDE}B^{ABC}(q_1, |\mathbf{k}_1-\mathbf{q}_1|, k)C^{DE}(q_2) \\
& +\frac{1}{4}N_A N_{BCDEF}C^{AB}(k)C^{CD}(q_1)C^{EF}(q_2)+\frac{1}{4}N_{ABC}N_{DEF}C^{AD}(k)C^{BC}(q_1)C^{EF}(q_2) \\
& +\frac{1}{2}N_{ABCD}N_{EF}C^{AB}(q_1)C^{CE}(|\mathbf{k}_1-\mathbf{q}_2|)C^{DF}(q_2) \\
& \left.+\frac{1}{6}N_{ABC}N_{DEF}C^{AD}(q_1)C^{BE}(|\mathbf{q}_2-\mathbf{q}_1|)C^{CF}(|\mathbf{q}_2-\mathbf{k}_1|)\right)\,. \qquad (35)
\end{aligned}$$

The final four terms were already shown diagrammatically in Fig. 4, they correspond to the last four terms of (35). However the mathematical expressions for these four diagrams given in (16) are correct at leading order in slow roll, while the expression above is valid to all orders in slow roll. Note that 1 of the 1 loop diagrams and 4 of the 2 loop diagrams have dressed vertices, these can be removed by renormalising the vertices in a similar way to the case with Gaussian fields, see App. A 2.

B. Trispectrum

The connected part of the primordial trispectrum is defined by

$$\langle \zeta_{\mathbf{k}_1}\,\zeta_{\mathbf{k}_2}\,\zeta_{\mathbf{k}_3}\,\zeta_{\mathbf{k}_4}\rangle_c \equiv T_\zeta(\mathbf{k}_1, \mathbf{k}_2, \mathbf{k}_3, \mathbf{k}_4)(2\pi)^3\delta^3(\mathbf{k_1}+\mathbf{k_2}+\mathbf{k_3}+\mathbf{k_4})\,. \qquad (36)$$

Diagrammatically all of the tree level terms for the 4-point function are given by Fig. 12. Writing down these terms in order we get

$$\begin{aligned}
T_\zeta^{\text{tree}}(\mathbf{k}_1, \mathbf{k}_2, \mathbf{k}_3, \mathbf{k}_4) \;=\; & N_A N_B N_C N_D T^{ABCD}(\mathbf{k}_1, \mathbf{k}_2, \mathbf{k}_3, \mathbf{k}_4) \\
& +N_{AB}N_C N_D N_E\left(C^{AC}(k_1)B^{BDE}(|\mathbf{k}_1+\mathbf{k}_2|, k_3, k_4)+(11\text{ perms})\right) \\
& +N_{AB}N_{CD}N_E N_F\left(C^{AC}(|\mathbf{k}_1+\mathbf{k}_3|)C^{BD}(k_3)C^{DF}(k_4)+(11\text{ perms})\right) \\
& +N_{ABC}N_D N_E N_F\left(C^{AD}(k_2)C^{BE}(k_3)C^{CF}(k_4)+(3\text{ perms})\right)\,. \qquad (37)
\end{aligned}$$

This result was first derived in [14, 41] without using diagrams (see also [27]). Note that all of the numerical coefficients are one, because all of the terms are tree level, and that only the final two terms are non-zero if the field fluctuations are Gaussian. The real space diagrams for these two terms were given in Fig. 1.

VI. CONCLUSION

We have presented a diagrammatic method for calculating any n-point function of the primordial curvature perturbation, ζ, at tree-level or any required loop level. Rules are given for first drawing diagrams at the required order, and then for writing down the corresponding terms in the n-point function, in either real or Fourier space. For example, we have drawn diagrams corresponding to all the 1- and 2-loop terms to the power spectrum and have given the corresponding corrections to the power spectrum.

Our method is based on using the δN-formalism which identifies the local curvature perturbation with the perturbation of the integrated expansion from an initial hypersurface. The expansion on large scales (typically larger than the Hubble scale) can be determined as a (non-linear) function of the initial local values of scalar fields during inflation using the homogeneous (FRW) equations of motion in the separate universe approach. In practice we are working with fields that are smoothed on scales $k > k_{\rm max} = (aH)_*$. In particular we neglect any ultraviolet divergence of the fields on small scales.

We show that it is possible to renormalise vertices by absorbing an infinite sum of terms, corresponding to loop corrections to vertices. These are automatically accounted for if we work in terms of the average local expansion $\langle N(\phi(\mathbf{x}))\rangle$ and its derivatives, defined in Eq. (25) for Gaussian fields, instead of the background expansion, $N(\phi_0)$. This removes terms such as $\langle\varphi^2\rangle$ which is divergent for scale-invariant spectra, leaving all n-point functions finite in real space so long as $\langle N(\phi(\mathbf{x}))\rangle$ and its derivatives are finite. However divergent terms remain in Fourier space due to integrals over loop momenta between vertices which may diverge in the infrared. A discussion of the effect of the large scale cut off on observables is given in [27, 42].[1]

Results for the primordial n-point function are given in terms of derivatives of N with respect to the fields at Hubble exit and the n-point functions of the fields evaluated at Hubble exit.

In single-field models of inflation the curvature perturbation is constant on super Hubble scales, so it is possible to calculate the derivatives of N explicitly at Hubble exit during inflation [14] without needing to know the details of the end of inflation or reheating, etc. In this case both the bispectrum and trispectrum have been shown to be small, regardless of whether the fields are assumed to be Gaussian or not, but assuming the field has a standard kinetic term in the action. During inflation the derivatives of N can be calculated explicitly even in multiple field models for a separable potential, this been done to second [44, 45, 46] and third order [41]. Several specific multiple field models have been studied in greater detail, e.g. $\mathcal{N}$-flation [47, 48] and a model of multiple field inflation in which N can be calculated exactly, [49]. For all examples considered so far in the slow roll regime the non-Gaussianity has proved to be small (see also [50, 51, 52]), however there are many models which explicitly generate a large non-Gaussianity after inflation. Examples include the curvaton scenario [6] and modulated reheating [53], also preheating, for example with hybrid inflation [54]. In general a numerical calculation of the derivatives of N is required, the advantage of the δN formalism is that we only need to solve the homogenous background equations.

If one assumes the fields are Gaussian then only the 2-point function of the fields is required, but in general one requires the $(r-1)$-point function of the fields when working to r'th order for any n-point function of ζ. So far the 3- and 4-point functions have been calculated, both at leading order in slow roll and ignoring any quantum mechanical loop corrections. It is possible but not expected that these corrections may be important [25, 55]. In the most commonly considered case of slow-roll inflation, the field is extremely close to Gaussian at Hubble exit so it is a good approximation to assume that the field is Gaussian and that any observable non-Gaussianity is generated after Hubble exit.

Methods to generate a large non-Gaussianity during inflation include having a break in the potential, [40], or to have a non-standard kinetic term so that the non-Gaussianity of the fields is large at Hubble exit [56], for example DBI inflation inspired from brane world models, [7].

Acknowledgments

The authors are grateful to David Lyth and Robert Crittenden for comments. KK is supported by PPARC (STFC). MS is supported in part by JSPS Grants-in-Aid for Scientific Research (A) No. 18204024 and (B) No. 1734007. The authors acknowledge support by the JSPS Japan-UK collaboration program.

[1] Two very recent papers which discuss this in depth are [37] by Lyth who estimates bounds on the size of the loop corrections to the 2-, 3- and 4-point functions and [26, 43] by Seery who more explicitly calculates the size of the one-loop contribution to the power spectrum. He finds that any large loop correction will come from the loop correction to the curvature perturbation on super Hubble scales rather then the quantum mechanical loop corrections on sub Hubble scales.

APPENDIX A: RENORMALISING DERIVATIVES OF N

Here we provide a proof that renormalising vertices removes the diagrams with dressed vertices. In real space this is equivalent to removing terms with $\langle\varphi^2\rangle$. We first provide a proof for the power spectrum where the notation is simpler. We then provide a proof for the general n-point function, initially assuming that the fields are Gaussian at Hubble exit, Sec. A 1, and finally extend this proof to allow for arbitrary field correlations at Hubble exit, Sec. A 2.

The gauge invariant curvature perturbation is defined by (2) as

$$\zeta = \delta N - \langle\delta N\rangle = \sum_{p=1}^{\infty}\frac{1}{p!}N_{\underbrace{AB\cdots C}_{p}}\left(\varphi^A\varphi^B\cdots\varphi^C - \langle\varphi^A\varphi^B\cdots\varphi^C\rangle\right)\,, \tag{A1}$$

where the subscript p means that there are p field indices above the brace. From the definition of ζ, the 2-point function is given by

$$\langle\zeta_x\zeta_y\rangle = \sum_{p,q=1}^{\infty}\frac{1}{p!q!}N_{\underbrace{AB\cdots C}_{p}}N_{\underbrace{DE\cdots F}_{q}}\langle\left(\varphi_x^A\varphi_x^B\cdots\varphi_x^C - \langle\varphi_x^A\varphi_x^B\cdots\varphi_x^C\rangle\right)\left(\varphi_y^D\varphi_y^E\cdots\varphi_y^F - \langle\varphi_y^D\cdots\varphi_y^F\rangle\right)\rangle\,. \tag{A2}$$

Because the fields are Gaussian every n-point function of the fields can be split into products of 2-point functions. We can choose the pairs to be connected pairs, i.e. each φ is evaluated at a different point or disconnected pairs which are $\langle\varphi^2\rangle$. We consider every possible way of splitting the term $\langle\varphi_x^A\varphi_x^B\cdots\varphi_x^C\varphi_y^D\varphi_y^E\cdots\varphi_y^F\rangle$ into pairs:

– Only disconnected pairs: this term vanishes from (A2) because we are working with ζ which satisfies $\langle\zeta\rangle = 0$.

– 1 connected pair: there are pq different ways to select this term. This gives

$$\sum_{p,q}\frac{pq}{p!q!}N_{\underbrace{AB\cdots C}_{p}}N_{\underbrace{DE\cdots F}_{q}}\delta^{AD}G(|x-y|)\langle\varphi_x^B\cdots\varphi_x^C\rangle\langle\varphi_y^E\cdots\varphi_y^F\rangle = \langle\tilde{N}_A\rangle\langle\tilde{N}^A\rangle G(|x-y|)\,, \tag{A3}$$

$$\text{where}\qquad \langle\tilde{N}_A\rangle = \sum_{p=1}^{\infty}\frac{1}{(p-1)!}N_{A\underbrace{B\cdots C}_{p-1}}\langle\varphi^B\cdots\varphi^C\rangle\,. \tag{A4}$$

– 2 connected pairs: there are $p(p-1)q(q-1)/2!$ ways to choose these two connected pairs. The factor of 2! comes because the order in which we pick the pairs does not matter. This gives

$$\begin{aligned}&\frac{1}{2!}\sum_{p,q}\frac{1}{(p-2)!(q-2)!}N_{AB\underbrace{\cdots C}_{p-2}}N_{DE\underbrace{\cdots F}_{q-2}}\delta^{AD}\delta^{BE}G^2(|x-y|)\langle\cdots\varphi_x^C\rangle\langle\cdots\varphi_y^F\rangle\\ =\;&\frac{1}{2!}\langle\tilde{N}_{AB}\rangle\langle\tilde{N}^{AB}\rangle G^2(|x-y|)\,.\end{aligned} \tag{A5}$$

Continuing this for every possible number of connected pairs, we find that (A2) is equivalent to

$$\langle\zeta_x\zeta_y\rangle = \sum_{r=1}^{\infty}\frac{1}{r!}\langle\tilde{N}_{\underbrace{AB\cdots C}_{r}}\rangle\langle\tilde{N}^{AB\cdots C}\rangle G^r(|x-y|)\,. \tag{A6}$$

1. General n-point function

From the definition of ζ the n-point function is given by

$$\begin{aligned}\langle\zeta_x\zeta_y\cdots\zeta_z\rangle \;=\; &\sum_{\underbrace{p,q,\ldots,r}_{n}}\frac{1}{p!q!\cdots r!}N_{\underbrace{AB\cdots C}_{p}}N_{\underbrace{DE\cdots F}_{q}}\cdots N_{\underbrace{GH\cdots I}_{r}}\\ &\times\langle\left(\varphi_x^A\varphi_x^B\cdots\varphi_x^C - \langle\varphi_x^A\varphi_x^B\cdots\varphi_x^C\rangle\right)\cdots\left(\varphi_z^G\varphi_z^H\cdots\varphi_z^I - \langle\varphi_z^G\varphi_z^H\cdots\varphi_z^I\rangle\right)\rangle\,.\end{aligned} \tag{A7}$$

Similar to the calculation of the 2-point function, we have to split the term $\langle\varphi_x^A\varphi_x^B\cdots\varphi_x^C\cdots\varphi_z^G\varphi_z^H\cdots\varphi_z^I\rangle$ into pairs in every possible way. In the case that some of the $x, y, \cdots z$ do not appear in a connected pair there is no

contribution to the n-point function, for example if φ_z terms do not appear in any connected terms then the last bracket of (A7) is $\left(\langle\varphi_z^G\varphi_z^H\cdots\varphi_z^I\rangle - \langle\varphi_z^G\varphi_z^H\cdots\varphi_z^I\rangle\right) = 0$. We are left with

$$\begin{aligned}\langle\zeta_x\zeta_y\cdots\zeta_z\rangle \;=\; & \sum_{\underbrace{p,q,\ldots r}_{n}} \frac{1}{p!q!\cdots r!} N_{\underbrace{AB\cdots C}_{p}} N_{\underbrace{DE\cdots F}_{q}} \cdots N_{\underbrace{GH\cdots I}_{r}} \\ & \times\langle\varphi_x^A\varphi_x^B\cdots\varphi_x^C\cdots\varphi_z^G\varphi_z^H\cdots\varphi_z^I\rangle_{cc}\,, \end{aligned} \tag{A8}$$

where the subscript cc to the angular brackets means that they must be decomposed into pairs such that every $x, y, \ldots, z$ appears in at least one connected pair. We introduce the notation that $l_{xy} \geq 0$ is the number of connected pairs of x and y and similarly for every other possible connected pair. Furthermore n_x is the number of φ_x that form part of a connected pair, so $n_x = l_{xy} + \cdots + l_{xz}$. Note that we require $1 \leq n_x \leq p$.

We consider a term in (A8) from an arbitrary choice of $l_{xy}, \cdots, l_{xz}$. The number of ways to choose the l_{xy} connected pairs of x, y correlators is given by $p(p-1)\cdots(p-l_{xy}+1)q\cdots(q-l_{xy}+1)/l_{xy}!$, then the number of ways to choose the l_{xz} connected correlators linking x and z is given by $(p-l_{xy})(p-l_{xy}-1)\cdots(p-l_{xy}-l_{xz}+1)\cdots r(r-1)\cdots(r-l_{xz}+1)/l_{xz}!$. Continuing this counting for all the pairs, we find the number of ways to split into the required number of connected pairs is

$$\frac{p(p-1)\cdots(p-n_x+1)\cdots r(r-1)\cdots(r-n_z+1)}{l_{xy}!l_{xz}!\cdots l_{yz}!}\,. \tag{A9}$$

This choice of $l_{xy}, \cdots, l_{yz}$ therefore gives the following term to (A7),

$$\begin{aligned} & \frac{1}{l_{xy}!\cdots l_{yz}!} \sum_{p,q,\ldots,r} \frac{1}{(p-n_x)!\cdots(r-n_z)!} N_{AB\cdots C} N_{DE\cdots F}\cdots N_{GH\cdots I}\delta^{AD}\delta^{BE}\cdots \\ & \times G^{l_{xy}}(|x-y|)\cdots G^{l_{yz}}(|y-z|)\underbrace{\langle\cdots\varphi_x^C\rangle}_{p-n_x}\cdots\underbrace{\langle\cdots\varphi_z^I\rangle}_{r-n_z} \end{aligned} \tag{A10}$$

$$= \frac{1}{l_{xy}!\cdots l_{yz}!}\langle\tilde{N}_{\underbrace{AB\cdots C}_{n_x}}\rangle\cdots\langle\tilde{N}_{\underbrace{GH\cdots I}_{n_z}}\rangle\delta^{AD}\delta^{BE}\cdots G^{l_{xy}}(|x-y|)\cdots G^{l_{yz}}(|y-z|)\,, \tag{A11}$$

where there are l_{xy} contraction of field indices of the first two factors of $\langle\tilde{N}_{AB\cdots C}\rangle$ etc. Repeating this for all allowed choices of $l_{xy}, \cdots, l_{yz}$ we get

$$\langle\zeta_x\zeta_y\cdots\zeta_z\rangle = \sum_{l_{xy},\cdots,l_{yz}} \frac{1}{l_{xy}!\cdots l_{yz}!}\langle\tilde{N}_{\underbrace{AB\cdots C}_{n_x}}\rangle\cdots\langle\tilde{N}_{\underbrace{GH\cdots I}_{n_z}}\rangle\delta^{AD}\delta^{BE}\cdots G^{l_{xy}}(|x-y|)\cdots G^{l_{yz}}(|y-z|)\,. \tag{A12}$$

Diagrammatically a term $G^{l_{xy}}(|x-y|)$ corresponds to l_{xy} propagators which all have both ends attached to the same spatial points x and y. This explains the numerical factor of $l_{xy}!$, as given by rule 5 in real space (or equivalently rule 6 in Fourier space).

2. Extension to non-Gaussian fields

Here we extend the proof that renormalising vertices eliminates the diagrams with dressed vertices also holds for non-Gaussian fields. By doing this we also derive the numerical factors that are associated with every diagram. The proof is more complex than before because we must consider every possible correlation of an arbitrary number of fields, rather than reducing every n-point correlation to products of 2-point functions. We now have

$$\begin{aligned}\langle\tilde{N}_{AB\cdots C}\rangle \;=\; & N_{AB\cdots C} + \frac{1}{2}N_{AB\cdots CDE}\langle\varphi^D\varphi^E\rangle + \frac{1}{3!}N_{AB\cdots CDEF}\langle\varphi^D\varphi^E\varphi^F\rangle \\ & + \frac{1}{4!}N_{AB\cdots CDEFG}\langle\varphi^D\varphi^E\varphi^F\varphi^G\rangle + \cdots\,. \end{aligned} \tag{A13}$$

The correlators here includes the connected and disconnected parts.

Again the n-point function of ζ is given by (A7) and we can reduce it to (A8) in a similar way to the case with Gaussian fields. However we now have to decompose the term in angle brackets into connected correlators of arbitrary order in every possible way. We extend the notation that l_{xy} is the number of terms like $\langle\varphi_x^A\varphi_y^B\rangle$ to more

general correlators like l_{xxzz} is the number of terms like $\langle\varphi_x^A\varphi_x^B\varphi_z^C\varphi_z^D\rangle_c$. Every l must have at least 2 distinct x_i in the subscript. We define n_x as the number of x's contained in the correlators and again we require that $1 \le n_x \le p$ and similarly for n_y, etc. We consider the term in (A8) coming from a particular choice of $l_{xy}, \cdots, l_{x\cdots x\cdots z}$, which we denote by

$$\begin{aligned} P^{A\cdots BC\cdots EF\cdots G\cdots H} &= \underbrace{\langle\varphi_x^A\varphi_y^E\rangle\cdots\langle\varphi_x^B\varphi_y^F\rangle}_{l_{xy}}\cdots\underbrace{\langle\varphi_x^C\cdots\varphi_x^D\cdots\varphi_z^G\rangle_c}_{l_{x\cdots x\cdots z}}\cdots\cdots \\ &= \prod\langle\underbrace{\varphi_x\cdots\varphi_x}_{p}\cdots\underbrace{\varphi_z\varphi\varphi_z}_{w}\rangle_c^{l_{x\cdots x\cdots z\cdots z}} \end{aligned} \tag{A14}$$

and the product on the last line is over all chosen correlators of the fields and we have also dropped the field indices on this line. We can repeat the calculation for the number of ways to split the total correlator of (A8) into the appropriate connected pairs. The only new point is that whenever an x_i appears more then once in the same $l_{x\cdots x\cdots z}$ the order in which we pick those x's does not matter, so we have to divide by the factorial of the number of x's raised to the power $l_{x\cdots x\cdots z}$. In total we get

$$\frac{p(p-1)\cdots(p-n_x+1)\cdots r(r-1)\cdots(r-n_z+1)}{\prod l_{x\cdots x\cdots z}!(u!\cdots w!)^{l_{x\cdots x\cdots z}}}\,, \tag{A15}$$

where the product in the denominator is over all l's and the number of x_i's repeated in each individual l.

Therefore this choice of l's gives the following contribution to (A7),

$$\begin{aligned} &\frac{1}{\prod l_{x\cdots x\cdots z}!(u!\cdots w!)^{l_{x\cdots x\cdots z}}}\sum_{p,q,\cdots,r}\frac{1}{(p-n_x)!\cdots(r-n_z)!}N_{AB\cdots C}N_{DE\cdots F}\cdots N_{GH\cdots I} \\ &\times P^{AB\cdots GH}\underbrace{\langle\cdots\varphi_x^C\rangle}_{p-n_x}\cdots\underbrace{\langle\cdots\varphi_z^I\rangle}_{r-n_z} \end{aligned} \tag{A16}$$

$$= \frac{1}{\prod l_{x\cdots x\cdots z}!(u!\cdots w!)^{l_{x\cdots x\cdots z}}}\langle\tilde{N}\underbrace{AB\cdots C}_{n_x}\rangle\cdots\langle\tilde{N}\underbrace{GH\cdots I}_{n_z}\rangle P^{AB\cdots GH}\,. \tag{A17}$$

Repeating this for all allowed choices of the l's this gives

$$\langle\zeta_x\zeta_y\cdots\zeta_z\rangle = \sum_{l_{xy},\cdots,l_{x\cdots x\cdots z}}\frac{1}{\prod l_{x\cdots x\cdots z}!(u!\cdots w!)^{l_{x\cdots x\cdots z}}}\langle\tilde{N}\underbrace{AB\cdots C}_{n_x}\rangle\cdots\langle\tilde{N}\underbrace{GH\cdots I}_{n_z}\rangle P^{AB\cdots I}\,. \tag{A18}$$

Eq. (A18) explains the numerical factor of rule 7 in Sec. V, except for the case of dressed vertices. The numerical factor for dressed vertices requires a calculation of the number of ways to reduce the n-point function in (A13) into connected pairs of the required order. If l correlators of order n each dress the same vertex then we need to know the number of ways to split the ln-point function into l lots of connected n-point functions. The result is

$$\frac{1}{l!}{}^{ln}C_n\,{}^{n(l-1)}C_n\cdots{}^{2n}C_n = \frac{(ln)!}{l!(n!)^l}\,, \tag{A19}$$

where the denominator of $l!$ arises because the order in which we pick the n-point functions does not matter. The factor of $(ln)!$ is cancelled by the numerical factor in (A13). The generalisation to more complicated dressed vertices is straightforward to calculate, for example the number of ways to split an $(n_1l_1+n_2l_2)$-point function into l_1 lots of connected n_1-point functions and l_2 lots of connected n_2-point functions is

$$\frac{1}{l_1!l_2!}\frac{(l_1n_1+l_2n_2)!}{(n_1!)^{l_1}(n_2!)^{l_2}}\,. \tag{A20}$$

In Fig. 13 we give two examples of these rules, both of which are 4 loop terms of the dressed vertex of $\tilde{N}_A$, the first diagram has $l=2$ and $n=3$ while the second diagram has $l_1=2, n_1=2, l_2=1$ and $n_2=3$. The associated mathematical expressions are

$$\frac{1}{2!3!^2}N_{ABCDEFG}\langle\varphi^B\varphi^C\varphi^D\rangle\langle\varphi^E\varphi^F\varphi^G\rangle\,, \tag{A21}$$

$$\frac{1}{2!2!^23!}N_{ABCDEFGH}\langle\varphi^B\varphi^C\rangle\langle\varphi^D\varphi^E\rangle\langle\varphi^F\varphi^G\varphi^H\rangle\,. \tag{A22}$$

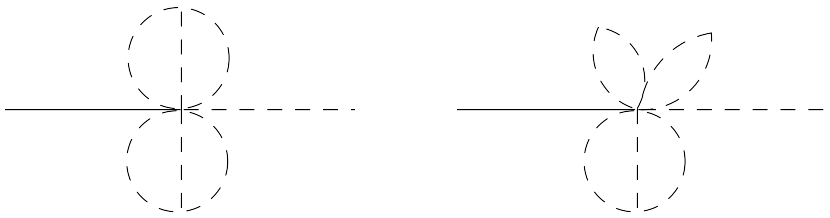

FIG. 13: Two terms of the renormalised vertex $\langle \tilde{N}_A \rangle$.

[1] www.hep.upenn.edu/ angelica/act/index.html
[2] www.rssd.esa.int/index.php?project=PLANCK
[3] V. Acquaviva, N. Bartolo, S. Matarrese and A. Riotto, Nucl. Phys. B **667**, 119 (2003) [arXiv:astro-ph/0209156].
[4] J. M. Maldacena, JHEP **0305**, 013 (2003) [arXiv:astro-ph/0210603].
[5] B. A. Bassett, S. Tsujikawa and D. Wands, Rev. Mod. Phys. **78**, 537 (2006) [arXiv:astro-ph/0507632].
[6] K. Enqvist and M. S. Sloth, Nucl. Phys. B **626**, 395 (2002) [arXiv:hep-ph/0109214]; D. H. Lyth and D. Wands, Phys. Lett. B **524**, 5 (2002) [arXiv:hep-ph/0110002]; T. Moroi and T. Takahashi, Phys. Lett. B **522**, 215 (2001) [Erratum-ibid. B **539**, 303 (2002)] [arXiv:hep-ph/0110096]; K. Enqvist and S. Nurmi, JCAP **0510**, 013 (2005) [arXiv:astro-ph/0508573]; K. A. Malik and D. H. Lyth, JCAP **0609**, 008 (2006) [arXiv:astro-ph/0604387]; M. Sasaki, J. Valiviita and D. Wands, Phys. Rev. D **74**, 103003 (2006) [arXiv:astro-ph/0607627].
[7] E. Silverstein and D. Tong, Phys. Rev. D **70**, 103505 (2004) [arXiv:hep-th/0310221]; M. Alishahiha, E. Silverstein and D. Tong, Phys. Rev. D **70**, 123505 (2004) [arXiv:hep-th/0404084]; M. x. Huang and G. Shiu, Phys. Rev. D **74**, 121301 (2006) [arXiv:hep-th/0610235].
[8] L. Verde, L. M. Wang, A. Heavens and M. Kamionkowski, Mon. Not. Roy. Astron. Soc. **313**, L141 (2000) [arXiv:astro-ph/9906301].
[9] L. M. Wang and M. Kamionkowski, Phys. Rev. D **61**, 063504 (2000) [arXiv:astro-ph/9907431].
[10] E. Komatsu and D. N. Spergel, Phys. Rev. D **63**, 063002 (2001) [arXiv:astro-ph/0005036].
[11] T. Okamoto and W. Hu, Phys. Rev. D **66**, 063008 (2002) [arXiv:astro-ph/0206155].
[12] N. Bartolo, S. Matarrese and A. Riotto, JCAP **0508**, 010 (2005) [arXiv:astro-ph/0506410].
[13] N. Kogo and E. Komatsu, Phys. Rev. D **73**, 083007 (2006) [arXiv:astro-ph/0602099].
[14] C. T. Byrnes, M. Sasaki and D. Wands, Phys. Rev. D **74**, 123519 (2006) [arXiv:astro-ph/0611075].
[15] A. A. Starobinsky, JETP Lett. **42**, 152 (1985) [Pisma Zh. Eksp. Teor. Fiz. **42**, 124 (1985)].
[16] M. Sasaki and E. D. Stewart, Prog. Theor. Phys. **95**, 71 (1996) [arXiv:astro-ph/9507001].
[17] D. H. Lyth, K. A. Malik and M. Sasaki, JCAP **0505**, 004 (2005) [arXiv:astro-ph/0411220].
[18] D. H. Lyth and Y. Rodriguez, Phys. Rev. Lett. **95**, 121302 (2005) [arXiv:astro-ph/0504045].
[19] D. S. Salopek and J. R. Bond, Phys. Rev. D **42**, 3936 (1990).
[20] M. Sasaki and T. Tanaka, Prog. Theor. Phys. **99**, 763 (1998) [arXiv:gr-qc/9801017].
[21] D. Wands, K. A. Malik, D. H. Lyth and A. R. Liddle, Phys. Rev. D **62**, 043527 (2000) [arXiv:astro-ph/0003278].
[22] R. Scoccimarro and J. Frieman, Astrophys. J. Suppl. **105**, 37 (1996) [arXiv:astro-ph/9509047].
[23] M. Crocce and R. Scoccimarro, Phys. Rev. D **73**, 063519 (2006) [arXiv:astro-ph/0509418].
[24] I. Zaballa, Y. Rodriguez and D. H. Lyth, JCAP **0606**, 013 (2006) [arXiv:astro-ph/0603534].
[25] M. S. Sloth, Nucl. Phys. B **748**, 149 (2006) [arXiv:astro-ph/0604488].
[26] D. Seery, arXiv:0707.3378 [astro-ph].
[27] L. Boubekeur and D. H. Lyth, Phys. Rev. D **73**, 021301 (2006) [arXiv:astro-ph/0504046].
[28] M. Musso, arXiv:hep-th/0611258.
[29] M. x. Huang, G. Shiu and B. Underwood, arXiv:0709.3299 [hep-th].
[30] D. Seery and J. E. Lidsey, JCAP **0509**, 011 (2005) [arXiv:astro-ph/0506056].
[31] D. Seery, J. E. Lidsey and M. S. Sloth, JCAP **0701**, 027 (2007) [arXiv:astro-ph/0610210].
[32] B. J. W. van Tent, Class. Quant. Grav. **21**, 349 (2004) [arXiv:astro-ph/0307048].
[33] C. T. Byrnes and D. Wands, Phys. Rev. D **74**, 043529 (2006) [arXiv:astro-ph/0605679].
[34] P. R. Jarnhus and M. S. Sloth, arXiv:0709.2708 [hep-th].
[35] D. H. Lyth and I. Zaballa, JCAP **0510**, 005 (2005) [arXiv:astro-ph/0507608].
[36] D. Binosi and L. Theussl, Comput. Phys. Commun. **161**, 76 (2004) [arXiv:hep-ph/0309015].
[37] D. H. Lyth, arXiv:0707.0361 [astro-ph].
[38] D. N. Spergel *et al.* [WMAP Collaboration], Astrophys. J. Suppl. **170**, 377 (2007) [arXiv:astro-ph/0603449].
[39] M. Sasaki, J. Valiviita and D. Wands, Phys. Rev. D **74**, 103003 (2006) [arXiv:astro-ph/0607627].
[40] X. Chen, R. Easther and E. A. Lim, JCAP **0706**, 023 (2007) [arXiv:astro-ph/0611645].
[41] D. Seery and J. E. Lidsey, JCAP **0701**, 008 (2007) [arXiv:astro-ph/0611034].
[42] D. H. Lyth, JCAP **0606**, 015 (2006) [arXiv:astro-ph/0602285].
[43] D. Seery, arXiv:0707.3377 [astro-ph].

[44] F. Vernizzi and D. Wands, JCAP **0605**, 019 (2006) [arXiv:astro-ph/0603799].
[45] T. Battefeld and R. Easther, JCAP **0703**, 020 (2007) [arXiv:astro-ph/0610296].
[46] K. Y. Choi, L. M. H. Hall and C. van de Bruck, JCAP **0702**, 029 (2007) [arXiv:astro-ph/0701247].
[47] S. A. Kim and A. R. Liddle, Phys. Rev. D **74**, 063522 (2006) [arXiv:astro-ph/0608186].
[48] D. Battefeld and T. Battefeld, JCAP **0705**, 012 (2007) [arXiv:hep-th/0703012].
[49] M. Sasaki, Class. Quant. Grav. **24**, 2433 (2007) [arXiv:astro-ph/0702182].
[50] L. Alabidi and D. H. Lyth, JCAP **0605**, 016 (2006) [arXiv:astro-ph/0510441].
[51] G. I. Rigopoulos, E. P. S. Shellard and B. J. W. van Tent, arXiv:astro-ph/0511041.
[52] S. Yokoyama, T. Suyama and T. Tanaka, arXiv:0705.3178 [astro-ph].
[53] G. Dvali, A. Gruzinov and M. Zaldarriaga, Phys. Rev. D **69**, 023505 (2004) [arXiv:astro-ph/0303591]; L. Kofman, arXiv:astro-ph/0303614.
[54] N. Barnaby and J. M. Cline, Phys. Rev. D **73**, 106012 (2006) [arXiv:astro-ph/0601481]; N. Barnaby and J. M. Cline, Phys. Rev. D **75**, 086004 (2007) [arXiv:astro-ph/0611750].
[55] S. Weinberg, Phys. Rev. D **74**, 023508 (2006) [arXiv:hep-th/0605244].
[56] X. Chen, M. x. Huang, S. Kachru and G. Shiu, JCAP **0701**, 002 (2007) [arXiv:hep-th/0605045].